Coronal equilibrium of high-atomic-number plasmas

David Mosher
Plasma Physics Division, Naval Research Laboratory, Washington, D. C. 20375
(Received 14 August 1974)

The distribution of ionization states in carbon, aluminum, copper, and tungsten plasmas is determined from the corona-model equilibrium. The variations of mean ionization level, internal energy, and radiation rates for continuum and lines with temperature are then determined by averaging over the ionization states. Results can be applied to studies of a variety of existing laboratory plasmas and to analyses of the effects of impurities in fusion plasmas.

The Saha equation, because of its simplicity, is commonly used to determine the equilibrium distribution of ionization states in nonhydrogenic plasmas.[1] However, plasmas of interest are frequently too high in temperature and insufficiently dense to satisfy the constraint of local thermodynamic equilibrium required for proper application of the Saha equation.[2] Plasmas which are predominantly transparent to their emitted radiation are more accurately characterized by the corona-model steady state for which the distribution of ionization levels is determined by a balance between collisional ionization and radiative recombination.[2] Here, we summarize results of calculations based on the corona model which parameterize the ionization-dependent properties and radiation rates of high-atomic-number plasmas. Specifically, the variations of mean ionization level, internal energy, and radiation rates with temperature are presented for carbon, aluminum, copper, and tungsten plasmas. A digital computer program, CORONA, was used to determine the distribution of ionization states. Appropriately weighted averages over the distribution yielded the macroscopic quantities of interest. Results can be applied to studies of a variety of existing laboratory plasmas and to analyses of the effects of impurities in proposed fusion-reactor plasmas.

The parameters of plasmas which can be characterized by coronal equilibrium are subject to a number of constraints, two of which are now presented. A more complete discussion of these requirements is presented elsewhere.[2] First, radiative recombination dominates three-body recombination when the electron density n_e satisfies the relation

$$n_e < 10^{16}\theta^{7/2}\ \mathrm{cm}^{-3}, \tag{1}$$

where θ is the electron temperature in eV. The second assumption is that the plasma is in a state of ionization equilibrium. This requires that the relaxation time for important atomic processes be short compared to the time τ over which the macroscopic plasma parameters vary. This condition is fulfilled if the electron density satisfies

$$n_e \gtrsim 10^{12}/\tau\ \mathrm{cm}^{-3}, \tag{2}$$

with τ in seconds. Equation (1) is satisfied for all plasmas of current interest while the second relation is satisfied for two distinct classes of plasmas. The first class includes high-energy-density, high-atomic-number plasmas such as those produced in a vacuum spark[3] and dense plasma focus,[4] or from the explosion of fine wires by high-power (10^{12} W) pulse generators.[5] The second class includes proposed fusion-reactor plasmas since Eq. (2) must be satisfied if Lawson's criterion is also to be met. The results to be presented are then useful for analyzing the effects of impurities in fusion plasmas with the possible exception of those formed by the laser-driven implosion of small masses of fusionable material.

The dominant ionization and recombination processes for a plasma in coronal equilibrium are both two body. The distribution of ionization levels determined by the balance of these two processes is thus independent of density; it is characterized solely by the local electron temperature θ and the atomic properties of the species under consideration.

The fraction f_Z of atoms of a given species which are Z-times ionized may be determined from the set of relations

$$\alpha_Z f_Z = S_{Z-1} f_{Z-1}, \quad 1 \le Z \le Z_j. \tag{3}$$

Here, α_Z is the recombination rate for a Z-times ionized atom, S_Z is the ionization rate, and Z_j is the atomic number of the atom. The solution of this set may be written

$$f_Z = (S_0/\alpha_1)(S_1/\alpha_2)\cdots(S_{Z-1}/\alpha_Z) f_0,$$
$$f_0 = \left(1 + \sum_{Z=1}^{Z_j} (S_0/\alpha_1)(S_1/\alpha_2)\cdots(S_{Z-1}/\alpha_Z)\right)^{-1}. \tag{4}$$

The quantities in the small parenthesis may be determined from[2]

$$\alpha_{Z+1}/S_Z = 7.87\times10^{-9}(\chi_Z^2/\eta_Z)(\chi_Z/\theta)^{3/4}e^{\chi_Z/\theta}. \quad (5)$$

In Eq. (5), χ_Z is the ionization potential in eV for ions in state Z going to $Z+1$ and η_Z is the number of outer-shell electrons in state Z. The quantities χ_Z are determined in calculations by Carlson *et al.*[6] The distributions of ionization states for carbon, aluminum, copper, and tungsten plasmas (covering the range of atomic numbers from 6 to 74) and selected values of θ are shown in Figs. 1(a)–1(d).

Since f_Z is determined from only elemental atomic properties and the electron temperature, macroscopic quantities obtained from appropriately weighted averages of f_Z over Z depend only on θ. The macroscopic quantities of interest are: the mean ionization level, the internal energy of the plasma including energy stored in ionization, and radiation rates for continuum and lines. The values of these quantities are now calculated assuming ions and electrons to be at the same temperature θ. Corrections due to ions at a temperature different from θ will be considered as required.

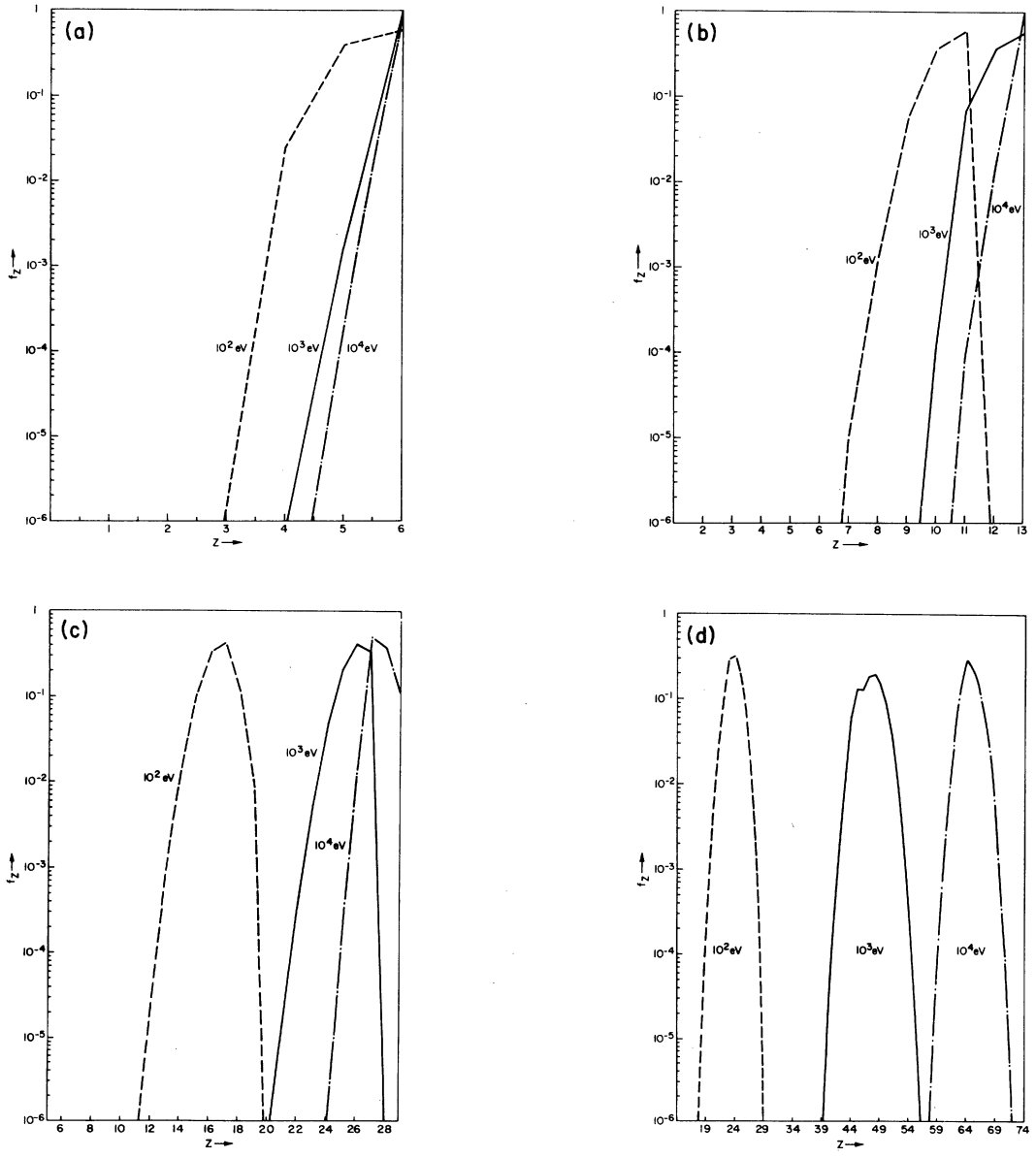

FIG. 1. (a) Distribution of ionization states for carbon ($Z_M=6$); (b) distribution of ionization states for aluminum ($Z_M=13$); (c) distribution of ionization states for copper ($Z_M=29$); (d) distribution of ionization states for tungsten ($Z_M=74$).

The thermal energy density associated with a plasma of species j at temperature θ is given by

$$h_j = \tfrac{3}{2}(n_j + n_{ej})\theta \text{ eV/cm}^3 ,$$

where n_j is the atomic density and n_{ej} is the contribution to the total electron density due to species j,

$$n_{ej} = \sum_{Z=0}^{Z_j} Z n_Z ; \quad n_e = \sum_j n_{ej} . \tag{6}$$

Here, n_Z is the density of Z-times ionized atoms,

$$n_Z = f_Z n_j .$$

It is understood that Z-dependent quantities (n_Z, f_Z, χ_Z, etc.) refer to a particular species.

Equation (6) may be written in the form

$$n_{ej} = \langle Z \rangle n_j , \tag{7}$$

where $\langle\ \rangle$ indicates an average over ionization states. For any Z-dependent quantity Ψ_Z

$$\langle \Psi \rangle = \sum_{Z=0}^{Z_j} f_Z \Psi_Z .$$

The variation of the mean ionization level $\langle Z \rangle$ with θ is shown in Fig. 2.

The energy per unit volume needed to ionize to equilibrium at temperature θ is given by

$$E_{Ij} = \sum_Z E_Z n_Z = \langle E_Z \rangle n_j \text{ eV/cm}^3 , \tag{8}$$

where E_Z is the energy required to ionize an atom from the neutral state to the Z-times ionized state

$$E_Z = \sum_{k=0}^{Z-1} \chi_k .$$

The total internal energy density associated with species j is then

$$h_j + E_{Ij} = [\tfrac{3}{2}(1 + \langle Z \rangle) + \langle E_Z \rangle / \theta] n_j \theta \text{ eV/cm}^3 . \tag{9}$$

The variation of the quantity in square brackets (the effective specific heat per atom) with θ is

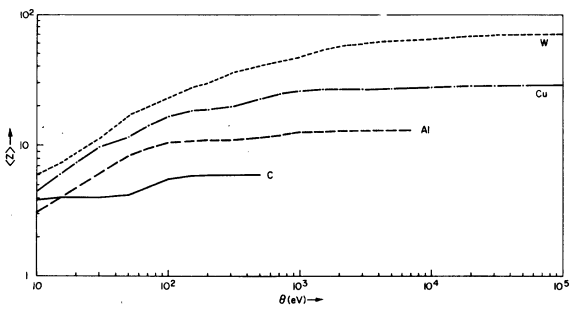

FIG. 2. Mean ionization level vs plasma temperature.

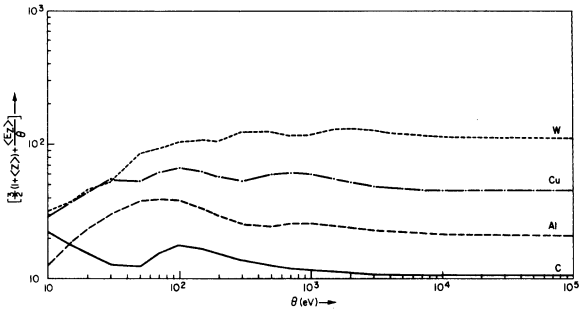

FIG. 3. Specific heat per atom vs plasma temperature.

shown in Fig. 3. If ions are at temperature θ_j

$$h_j + E_{Ij} = [\tfrac{3}{2}\theta_j + (C_j - \tfrac{3}{2})\theta] n_j \text{ eV/cm}^3 , \tag{10}$$

where

$$C_j = \tfrac{3}{2}(1 + \langle Z \rangle) + \langle E_Z \rangle / \theta .$$

The power density of free-free bremsstrahlung radiation due to elastic electron collisions with ions of density n_Z and charge Ze is given by[7]

$$P_Z = 1.5 \times 10^{-32} \theta^{1/2} n_e n_Z Z^2 \text{ W/cm}^3 .$$

The total free-free emission for species j due to the various ionization states is then

$$P_{ff} = \sum_{Z=0}^{Z_j} P_Z = 1.5 \times 10^{-32} \theta^{1/2} \langle Z^2 \rangle n_j n_e \text{ W/cm}^3 . \tag{11}$$

For ions of charge Ze, the ratio of power emitted as recombination (free-bound) radiation to bremsstrahlung is[7] χ_{Z-1}/θ. The total continuum radiation may then be written as

$$P_{cj} = 1.5 \times 10^{-32} \theta^{1/2} n_j n_e (\langle Z^2 \rangle + \langle Z^2 \chi_{Z-1}/\theta \rangle) \text{ W/cm}^3 . \tag{12}$$

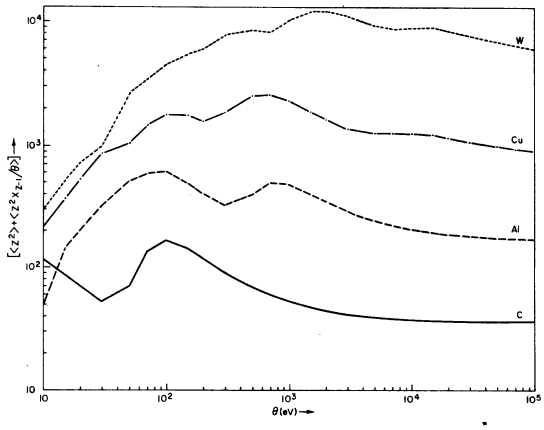

FIG. 4. Continuum radiation factor vs plasma temperature.

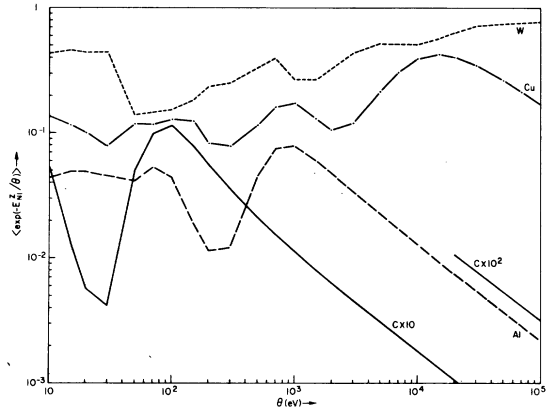

FIG. 5. Line radiation factor vs plasma temperature.

The variation of the quantity inside the parentheses with θ is shown in Fig. 4.

In the absence of radiation trapping, the power density of line radiation may be determined from[7]

$$P_L = 7\times 10^{-25}\theta^{-1/2} n_e \sum_{N,Z} g^Z_{Ni} n_Z e^{-E^Z_{Ni}/\theta} \text{ W/cm}^3 ,$$

where, consistent with the assumption of coronal equilibrium, radiative decay is taken to predominate over collisional deexcitation for lines.[8] Here, g^Z_{Ni} is the oscillator strength associated with the electron transition $N \to i$ with energy difference E^Z_{Ni} for an atom in ionization state Z.

Following Griem,[7] it is assumed that the only important transition is that for the resonance line $N \to N+1$ where N is the principle quantum number of an outer-shell electron in state Z, and that the oscillator strength is $\frac{1}{2}$ for this transition. These simplifications usually yield good approximations for the line-radiation rates since most energy radiated is typically in the resonance line.

The value of E^Z_{Ni} for this transition may be estimated from the Bohr theory

$$E^Z_{N,N+1} = (\alpha Z)^2 \frac{m_0 c^2}{2}\left(\frac{1}{N^2} - \frac{1}{(N+1)^2}\right),$$

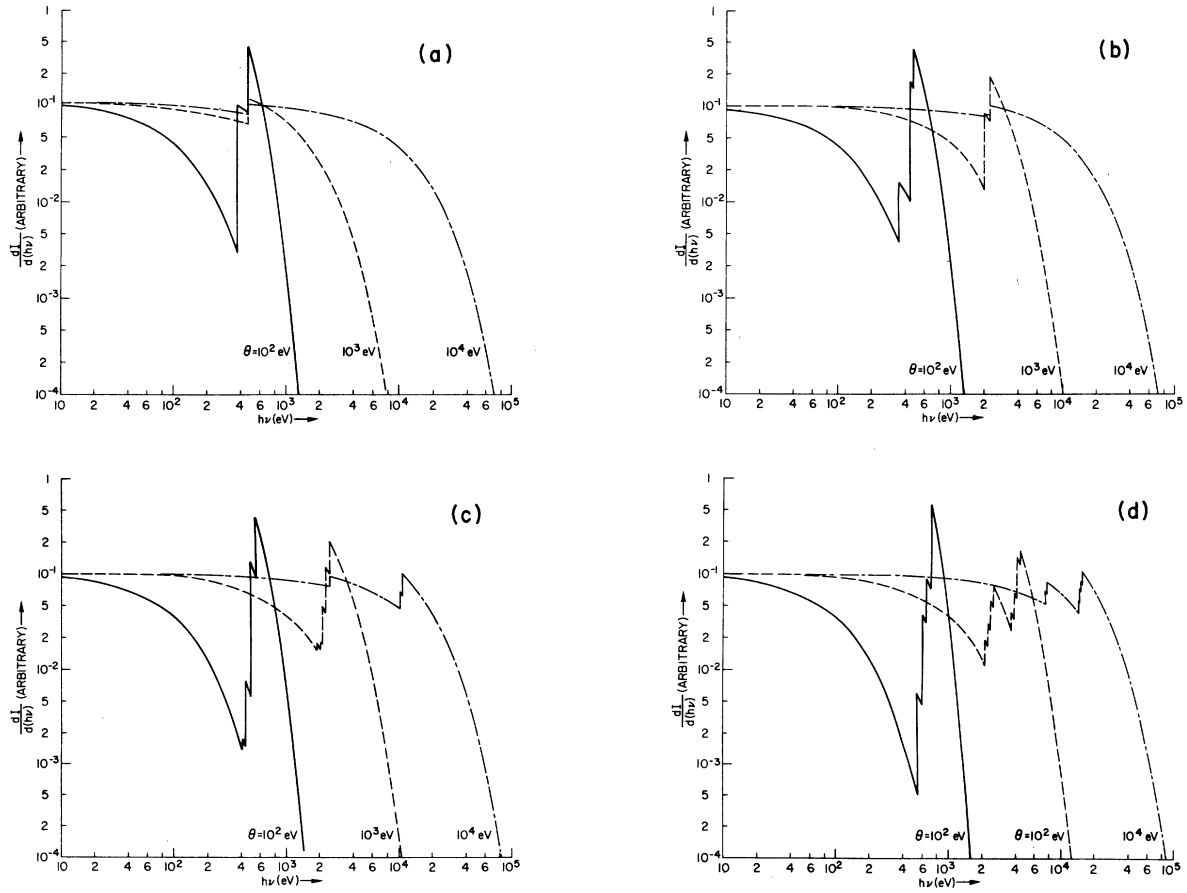

FIG. 6. (a) Continuum spectrum of carbon; (b) continuum spectrum of aluminum; (c) continuum spectrum of copper; (d) continuum spectrum of tungsten.

where α is the fine structure constant and m_0c^2 is the electron rest energy. The power density of line radiation may then be estimated from

$$P_L \approx 3.5\times10^{-25}\theta^{-1/2}n_j n_e \langle e^{-E^Z_{N,N+1}/\theta}\rangle \text{ W/cm}^3 . \quad (13)$$

The variation of the exponential term with θ is shown in Fig. 5.

The above radiation rates are correct only if the plasma may be considered optically thin to the bulk of the radiation. These rates are reduced when photon absorption lengths are less than, or comparable to, the dimensions of the plasma. Since the absorption coefficients for characteristic lines and continuum are different,[9,10] it may be important to maintain the distinction between the two types of radiation loss in low-temperature plasmas. Self-absorption of impurity radiation is certainly negligible in plasmas such as those proposed for Tokamak reactors ($n_e \approx 10^{14}/\text{cm}^3$, $\theta \approx 10^4$ eV). However, absorption of low-energy photons ($h\nu \lesssim 100$ eV) should be considered when modeling high-atomic-number, pulsed plasmas such as those created from exploded wires[5] ($n_e \gtrsim 10^{20}/\text{cm}^3$, $\theta \lesssim 10^3$ eV).

In addition to the total rate of energy loss due to radiation, it is of interest to determine the spectral character of radiation emitted by an isother-

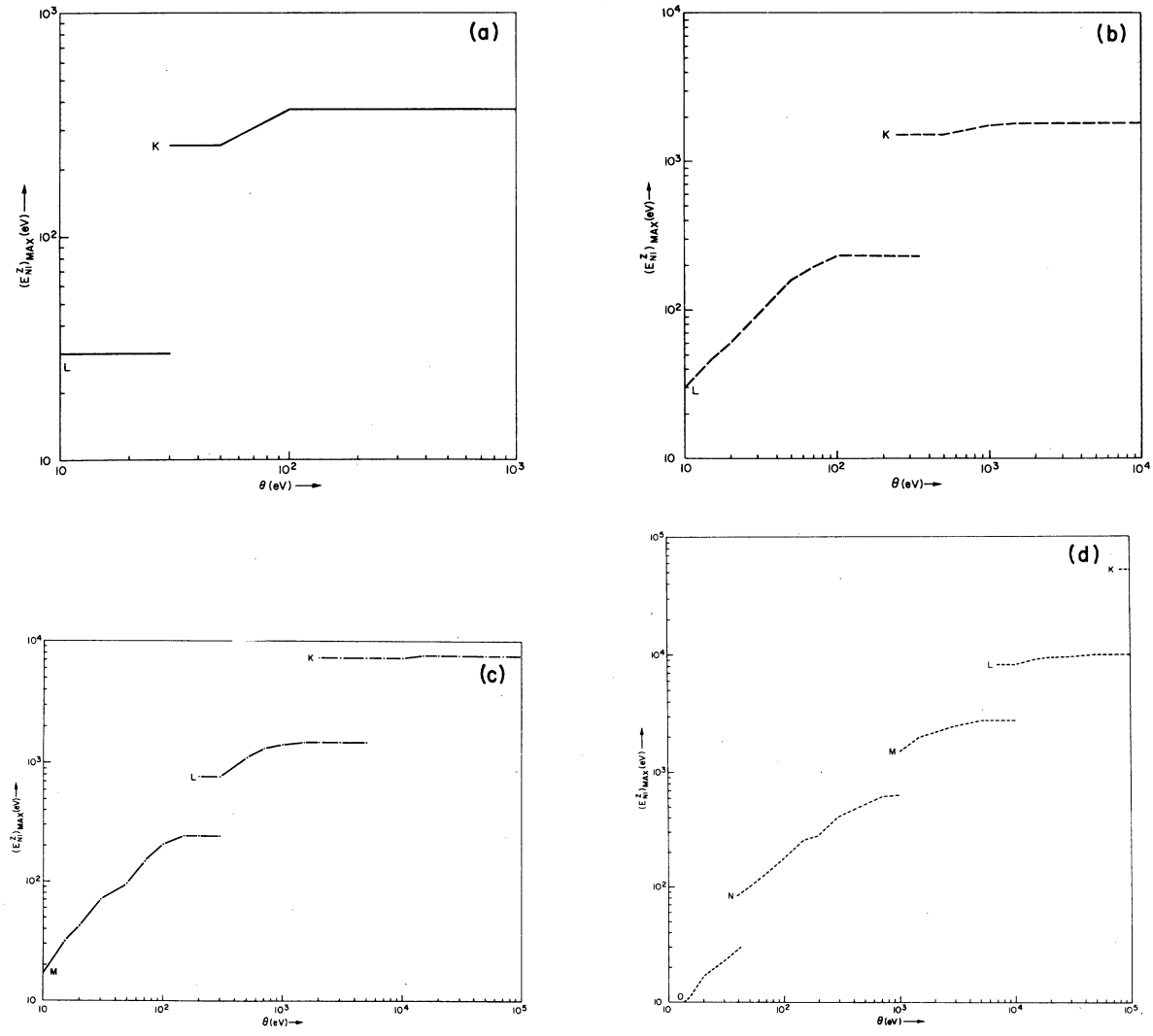

FIG. 7. (a) Photon energy of maximum intensity lines for carbon; (b) photon energy of maximum intensity lines for aluminum; (c) photon energy of maximum intensity lines for copper; (d) photon energy of maximum intensity lines for tungsten.

mal plasma. Knowledge of the theoretical continuum and line spectra allows one to: (a) determine the degree to which radiation is reabsorbed in a self-consistent fashion, and (b) estimate the temperature of a laboratory plasma by comparing experimental x-ray spectra with those predicted theoretically.

For a Boltzmann distribution of free electrons in a Z-times ionized plasma, the spectral intensities of free-free and free-bound radiation vary as[2]

$$\frac{dP_{ff}}{d(h\nu)} \sim e^{-h\nu/\theta}, \text{ all } h\nu;$$

$$\frac{dP_{fb}}{d(h\nu)} \sim e^{(\chi_{Z-1}-h\nu)/\theta}, \quad h\nu > \chi_{Z-1} . \tag{14}$$

Using the scaling provided by Eqs. (11), (12), and (14), and averaging over ionization states allows one to determine the continuum spectrum. Optically thin continuum spectra for carbon, aluminum, copper, and tungsten are shown in Figs. 6(a)–6(d) for selected values of θ.

The relative contribution of each line of energy $h\nu = E^Z_{N,N+1}$ to the total line-radiation loss rate can be estimated by calculating each element in the sum over Z in Eq. (13). The value of $h\nu$ for the dominant line is plotted against θ in Figs. 7(a)–7(d). Detailed line spectra cannot be determined from the theory employed here since all nonresonant and inner-shell transitions and orbital-electron shielding have been neglected.

ACKNOWLEDGMENTS

The author wishes to thank David Grubb and Michael Mussetto for their help with computer programming. The author is also grateful for useful discussions with Dr. Harold Epstein. This work was supported by the Defense Nuclear Agency.

[1]H. W. Drawin and P. Felenbok, *Data for Plasmas in Local Thermodynamic Equilibrium* (Gauthier-Villars, Paris, 1965).
[2]R. W. P. McWhirter and T. F. Stratton, in *Plasma Diagnostic Techniques*, edited by R. H. Huddlestone and S. L. Leonard (Academic, New York, 1965).
[3]T. N. Lie and R. C. Elton, Phys. Rev. A 3, 865 (1971).
[4]J. W. Mather *et al.*, Bull. Am. Phys. Soc. 18, 1363 (1973).
[5]D. Mosher *et al.*, Appl. Phys. Lett. 23, 429 (1973).
[6]T. A. Carlson, C. W. Nestor, Jr., N. Wasserman, and J. D. McDowell, At. Data 2, 1 (1970).
[7]H. R. Griem, *Plasma Spectroscopy* (McGraw-Hill, New York, 1964).
[8]J. Cooper, Rep. Prog. Phys. 29, 49 (1966).
[9]L. Spitzer, Jr., *Physics of Fully Ionized Gases* (Interscience, New York, 1962).
[10]R. C. Elton, in *Methods of Experimental Physics*, edited by H. R. Griem and R. H. Lovberg (Academic, New York, 1970).